Supplement of Weather Clim. Dynam., 7, 149–164, 2026
https://doi.org/10.5194/wcd-7-149-2026-supplement

Supplement of

Storylines of extreme summer temperatures in southern South America

Solange Suli et al.

Correspondence to: Solange Suli (ssuli@ucm.es)

Model name	Modelling centre	Member	Resolution (lon x lat)
ACCESS-CM2	Australian Community Climate and Earth System Simulator (ACCESS), Australia	r1i1p1f1	1.9º x 1.3º
ACCESS-ESM1-5	Australian Community Climate and Earth System Simulator (ACCESS), Australia	r1i1p1f1	1.9º x 1.3º
BCC-CSM2-MR	Beijing Climate Center, Beijing, China	r1i1p1f1	1.1º x 1.1º
CAMS-CSM1-0	Chinese Academy of Meteorological Sciences, Beijing, China	r2i1p1f1	1.1º x 1.1º
CMCC-ESM2	Fondazione Centro Euro-Mediterraneo sui Cambiamenti Climatici, Italy	r1i1p1f1	1.3º x 0.9º
CNRM-CM6-1	Centre National de Recherches Météorologiques, France	r1i1p1f2	1.4º x 1.4º
CNRM-CM6-1-HR	Centre National de Recherches Météorologiques, France	r1i1p1f2	0.5º x 0.5º
CNRM-ESM2-1	Centre National de Recherches Météorologiques, France	r1i1p1f2	1.4º x 1.4º
EC-Earth3	Consortium of various institutions from Spain, Italy, Denmark, Finland, Germany, Ireland, Portugal, Netherlands, Norway, the United Kingdom, Belgium, and Sweden	r1i1p1f1	0.7º x 0.7º
EC-Earth3-CC	Consortium of various institutions from Spain, Italy, Denmark, Finland, Germany, Ireland, Portugal, Netherlands, Norway, the United Kingdom, Belgium, and Sweden	r1i1p1f1	0.7º x 0.7º
EC-Earth3-Veg	Consortium of various institutions from Spain, Italy, Denmark, Finland, Germany, Ireland, Portugal, Netherlands, Norway, the United Kingdom, Belgium, and Sweden	r1i1p1f1	0.7º x 0.7º
EC-Earth3-Veg-LR	Consortium of various institutions from Spain, Italy, Denmark, Finland, Germany, Ireland, Portugal, Netherlands, Norway, the United Kingdom, Belgium, and Sweden	r1i1p1f1	1.1º x 1.1º
GFDL-CM4	National Oceanic and Atmospheric Administration, GFDL, Princeton, USA	r1i1p1f1	1.3º x 1.0º

GFDL-ESM4	National Oceanic and Atmospheric Administration, GFDL, Princeton, USA	r1i1p1f1	1.3º x 1.0º
GISS-E2-1-G	Goddard Institute for Space Studies, United States	r1i1p1f2	2.5º x 2º
HADGEM3-GC31-LL	Met Office Hadley Centre (UKMO), United Kingdom	r1i1p1f3	1.9º x 1.3º
HADGEM3-GC31-MM	Met Office Hadley Centre (UKMO), United Kingdom	r1i1p1f3	0.8 x 0.6
INM-CM4-8	Institute for Numerical Mathematics, Russian Academy of Science, Moscow, Russia	r1i1p1f1	2.0º x 1.5º
INM-CM5-0	Institute for Numerical Mathematics, Russian Academy of Science, Moscow, Russia	r1i1p1f1	2.0º x 1.5º
IPSL-CM6A-LR	Institut Pierre Simon Laplace, Paris, France	r1i1p1f1	2.5º x 1.3º
KACE-1-0-G	National Institute of Meteorological Sciences/Korea Meteorological Administration (NIMS-KMA), South Korea	r1i1p1f1	1.9º x 1.3º
MPI-ESM1-2-HR	Max Planck Institute for Meteorology, Germany	r1i1p1f1	0.9º x 0.9º
MPI-ESM1-2-LR	Max Planck Institute for Meteorology, Germany	r1i1p1f1	1.9º x 1.9º
MRI-ESM2-0	Meteorological Research Institute, Tsukuba, Japan	r1i1p1f1	1.1º x 1.1º
TAIESM1	Research Center for Environmental Changes, Academia Sinica, Taiwan	r1i1p1f1	1.3º x 0.9º
UKESM1-0-LL	Met Office Hadley Centre (UKMO), Devon, United Kingdom	r1i1p1f2	1.9º x 1.3º

Table S1. List of CMIP6 models used in the study.

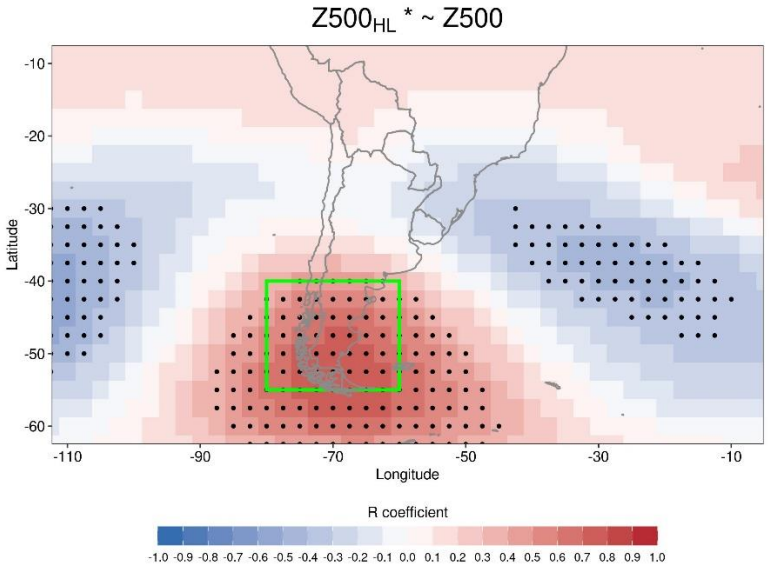

Figure S1. MMM Pearson correlation coefficients of the summer (DJF) series of the $Z500_{HL}$* driver and Z500 during the historical period (1979–2014). The box indicates the region used to construct the driver and stippling areas denote regions where at least 66% of the models show significant correlations ($p < 0.1$) of the same sign.

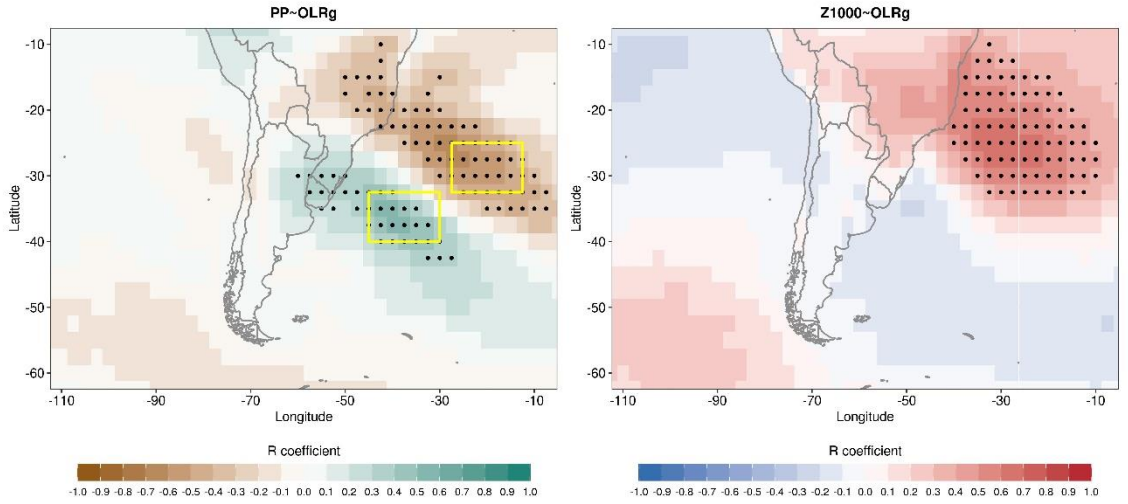

Figure S2. MMM Pearson correlation coefficients of the summer (DJF) series of the OLRg driver and 2D fields of: left) precipitation; right) Z1000 during the historical period (1979–2014). Boxes indicate the regions used to construct the OLR gradient and stippling areas denote regions where at least 66% of the models show significant correlations ($p < 0.1$) of the same sign.

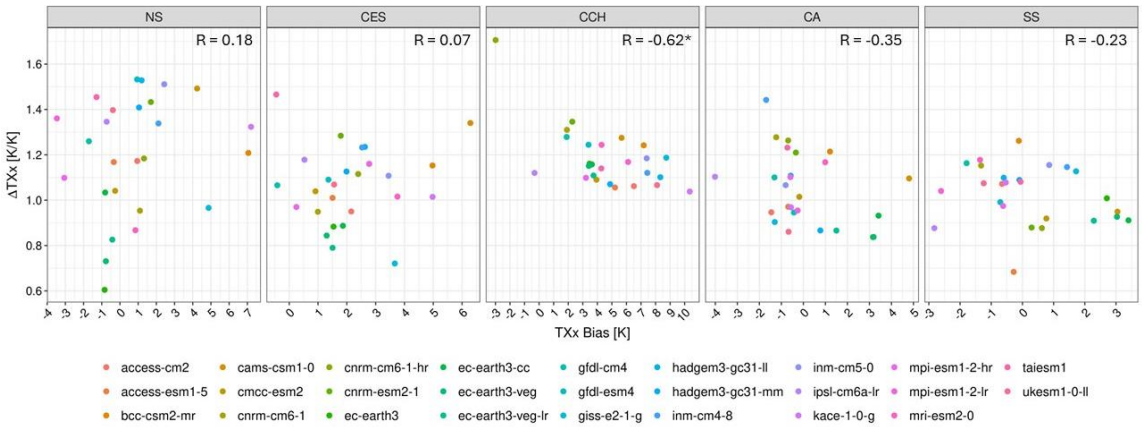

Figure S3. Summer TXx changes (ΔTXx) scaled by global warming (K/K) against TXx biases [K] for each GCM (colour circles) and SSA region (panels). The Pearson correlation coefficient is shown in the upper right corner, with an asterisk denoting statistically significant correlations at the 95% confidence level.

Driver	Internal variability	Inter-model spread	Inter-model spread / Internal variability
N3.4	0.07	0.45	6.42*
OLRg	3.13	13.55	4.32*
$Z500_{HL}$*	27.98	51.71	1.85*
SM_{SS}	0.06	0.78	13.00*
SM_{CA}	0.09	0.54	6.00*
SM_{north}	0.18	2.20	12.22*

Table S2. Internal variability (MMM standard deviation of the detrended series) and inter-model spread (standard deviation of the projected changes) for the selected drivers of each SSA region. All values are scaled by global warming. The last column represents the ratio of uncertainty to internal variability, with asterisks indicating significant differences at $p<0.1$ after an F-test.

Region	ΔTXx	ΔTX90	ΔD	ΔE	ΔI
NS	ΔN3.4, ΔOLRg	-	-	-	-
CES	ΔOLRg	-	-	ΔOLRg	-
CA	ΔSM_{CA}, ΔOLRg	ΔSM_{CA}	ΔSM_{CA}	ΔSM_{CA}, ΔOLRg	-
SS	ΔSM_{SS}, $\Delta Z500_{HL}^{*}$	$\Delta Z500_{HL}^{*}$	$\Delta Z500_{HL}^{*}$	ΔOLRg	ΔSM_{SS}

Table S3. Statistically significant drivers (p-value < 0.1) for each heatwave index (columns: ΔTXx, ΔTX90, and changes in duration, extension and intensity) and SSA region (rows: NS, CES, CA and SS). Heatwave attributes were extracted from the algorithm developed by Sánchez-Benítez et al. (2020). The dash ('-') indicates that none of the drivers showed a statistically significant relationship with the corresponding index.